



Forecasting and time variability analysis of Ozone concentrations using nitrate oxide and meteorological variables as predictors

This manuscript ([permalink](#)) was automatically generated from [uiceds/cee-492-term-project-fall-2022-hydrograds@031a31b](#) on December 4, 2022.

Authors

- **Jiewen Luo**
·  [Noomi-Luo](#)
Department of CEE, University of Illinois at Urbana&Champaign
- **Rourou Ji**
·  [Jadeji](#)
Department of CEE, University of Illinois at Urbana&Champaign
- **Bernardo Burbano**
·  [BernieJBA](#)
Department of CEE, University of Illinois at Urbana&Champaign

Introduction

The purpose of this project is to predict O_3 concentrations using measurements of concentration of other pollutants and available meteorological measurements. Ozone might be formed when heat and sunlight cause chemical reactions between oxides of nitrogen (NO_x) and Volatile Organic Compounds (VOC), which are also known as Hydrocarbons. Therefore it could be hypothesized that using measurements of NO_x as an independent variable a model could be developed to predict O_3 concentrations. Additionally, meteorological variables such as air temperature, relative humidity(RH) and ultraviolet index (UVB - UVI) could be included as independent variables to assess their influence on temporal variability of ozone.

The dataset used in this project is a CSV file about the air quality in northern Taiwan collected in 2015 [<https://www.kaggle.com/datasets/nelsonchu/air-quality-in-northern-taiwan>], which includes air quality data and meteorological monitoring data for research and analysis, originally from Environmental Protection Administration, Executive Yuan, R.O.C. (Taiwan). There are 25 observation stations in total. Columns in this CSV file are the following:

Time - The first column is the observation time of 2015

Station - The second column is the station name, there are 25 observation stations, those stations are showing at the Table 1 .

Items - From the third column to the last one

item - unit - description

SO2 - ppb - Sulfur dioxide

CO - ppm - Carbon monoxide

O3 - ppb - ozone

PM10 - $\mu\text{g}/\text{m}^3$ - Particulate matter

PM2.5 - $\mu\text{g}/\text{m}^3$ - Particulate matter

NOx - ppb- Nitrogen oxides

NO - ppb - Nitric oxide

NO2 - ppb - Nitrogen dioxide

THC - ppm - Total Hydrocarbons

NMHC - ppm - Non-Methane Hydrocarbon

CH4 - ppm - Methane

UVB - UVI - Ultraviolet index

AMB_TEMP - Celsius - Ambient air temperature

RAINFALL - mm

RH - % - Relative humidity

WIND_SPEED - m/sec - The average of the last ten minutes per hour

WIND_DIREC - degrees - The average of the last ten minutes per hour

WS_HR - m/sec - The average of an hour

WD_HR - degrees - The average of an hour

PH_RAIN - PH - Acid rain

RAIN_COND - $\mu\text{S}/\text{cm}$ - Conductivity of acid rain

Table 1: A table contain all stations in Taiwan.

		station		
Banqiao	Cailiao	Datong	Dayuan	Guanyin
Guting	Keelung	Longtan	Pingzhen	Sanchong
Shilin	Songshan	Tamsui	Taoyuan	Tucheng
Wanhua	Wanli	Xindian	Xinzhuang	Xizhi
Yangming	Yonghe	Zhongli	Zhongshan	Linkou

After the air quality data has been processed, the strongest O₃ predictors will be determined by using a correlation matrix, along with other additional steps involving the exploratory data analysis. Neural network and convolutional neural networks will be used to predict hourly concentrations of O₃. As and additional predictive model to be tested a LSTM (long short-term memory) neural network will used since the data is time dependent. All this different neural network architectures will be evaluated in terms of error metrics to determine which on is the most suitable to predict O₃ concentrations using the information available on the dataset.

Exploratory Data Analysis

In order to explore the relation between the dependent variable and independent variables several scatter plots were created between meteorological variables, pollutant concentrations and ozone concentrations. Additionally, a heatmap was generated to investigate the correlation values between ozone concentration and independent variables. The most correlated meteorological variables are RH(relative humidity) and UVB(Ultraviolet index). RH is negatively correlated with ozone,value of -0.51, while UVB is positively correlated, value of 0.51. Another relevant observation was that concentrations of nitrogen-containing chemicals compounds are highly correlated between each other, and also are among the most correlated variables with respect to the predictand (ozone).

Furthermore, the fraction of available measurements, meaning the number of data points available divided by the number of hours in a year, was computed for all stations and all measured variables. This computation helped visualize the stations that missed the least data points as well as the variables whose values are recorded the most consistently through different stations. The station with the highest fraction of available measurements was Banquiao, as seen in the Figure 1. For this reason the remaining portion of this EDA was devoted to this station. Other relevant statistics from the Banquiao air quality station are shown in the following Table 2.

	Dependent Variable	Independent variable: Nitrogen based					Independent variable: Metereological variables						
Station	O3	NMHC	NO	NO2	NOx	Temperature	RH	UVB	W Direction 10 min	W Speed 10min	W Speed hourly	Wind Direction hourly	Average Fraction
Banqiao	0.991	0.984	0.966	0.966	0.966	0.991	0.991	0.991	0.991	0.991	0.991	0.991	0.984
Cailliao	0.978	0.000	0.958	0.958	0.958	0.977	0.978	0.000	0.977	0.977	0.977	0.977	0.794
Dayuan	0.988	0.000	0.975	0.975	0.975	0.980	0.955	0.000	0.852	0.910	0.922	0.922	0.770
Guanyin	0.980	0.000	0.969	0.969	0.969	0.973	0.980	0.000	0.977	0.980	0.979	0.977	0.798
Guting	0.988	0.966	0.983	0.983	0.983	0.985	0.983	0.000	0.985	0.985	0.985	0.985	0.901
Keelung	0.987	0.970	0.977	0.977	0.977	0.977	0.980	0.000	0.986	0.986	0.986	0.986	0.891
Linkou	0.973	0.000	0.966	0.966	0.966	0.973	0.973	0.000	0.972	0.972	0.964	0.972	0.793
Longtan	0.982	0.000	0.961	0.961	0.961	0.982	0.982	0.000	0.982	0.982	0.981	0.981	0.798
Pingzhen	0.988	0.000	0.968	0.968	0.968	0.988	0.988	0.000	0.983	0.988	0.988	0.988	0.802
Shilin	0.983	0.000	0.957	0.957	0.957	0.983	0.983	0.000	0.983	0.983	0.980	0.983	0.797
Songshan	0.985	0.967	0.976	0.976	0.976	0.985	0.985	0.000	0.984	0.984	0.984	0.984	0.891
Tamsui	0.961	0.000	0.956	0.956	0.956	0.000	0.000	0.961	0.000	0.000	0.000	0.000	0.348
Taoyuan	0.983	0.958	0.976	0.976	0.976	0.982	0.982	0.976	0.982	0.982	0.982	0.982	0.978
Tucheng	0.981	0.974	0.965	0.965	0.965	0.980	0.981	0.000	0.980	0.980	0.980	0.980	0.886
Wanhua	0.986	0.000	0.979	0.979	0.979	0.986	0.986	0.000	0.986	0.986	0.986	0.986	0.805
Wanli	0.984	0.000	0.976	0.976	0.976	0.983	0.976	0.000	0.976	0.982	0.983	0.975	0.800
Xindian	0.985	0.000	0.979	0.979	0.979	0.985	0.982	0.000	0.985	0.985	0.985	0.985	0.804
Xinzhuang	0.978	0.000	0.970	0.970	0.970	0.978	0.978	0.000	0.978	0.978	0.978	0.978	0.798
Xizhi	0.963	0.000	0.954	0.954	0.954	0.962	0.962	0.000	0.962	0.962	0.958	0.958	0.784
Yangming	0.979	0.000	0.964	0.964	0.964	0.979	0.979	0.000	0.000	0.000	0.000	0.000	0.441
Yonghe	0.987	0.972	0.978	0.978	0.978	0.984	0.987	0.000	0.987	0.987	0.987	0.987	0.893
Zhongli	0.988	0.973	0.967	0.967	0.967	0.986	0.986	0.000	0.986	0.986	0.985	0.985	0.890
Zhongshan	0.986	0.976	0.976	0.976	0.976	0.986	0.986	0.000	0.986	0.986	0.986	0.986	0.893

Figure 1: Data availability of air quality stations

index	AMB_TEMP	NMHC	NO	NO2	NOx	O3	RH	UVB	WD_Hour	WIND_DIR EC_10min	WIND_SPEED _10min	WS_HR
std	5.72	0.19	8.74	10.38	16.35	19.41	11.94	2.24	92.38	92.94	1.12	1.03
min	10.00	0.00	-0.40	1.90	3.00	0.20	13.00	0.00	0.20	0.10	0.50	0.00
mean	24.11	0.25	6.16	22.05	28.20	26.44	70.95	1.24	145.83	145.47	2.10	1.72
max	37.00	3.27	212.00	79.00	268.00	144.00	99.00	12.00	360.00	360.00	11.00	9.80
count	8682.00	8619.00	8462.00	8462.00	8462.00	8685.00	8684.00	8684.00	8680.00	8682.00	8682.00	8680.00
75%	28.00	0.30	6.60	28.00	35.00	37.00	80.00	1.50	239.00	239.00	2.70	2.30
50%	25.00	0.19	3.40	21.00	25.00	25.00	73.00	0.00	91.00	92.00	1.90	1.60
25%	19.00	0.13	1.80	14.00	17.00	11.00	62.00	0.00	74.00	73.00	1.30	0.90

Figure 2: Statistics of air quality and relevant meteorological variables from Banqiao station

As described in previous sections, the dataset consists of hourly observations of ozone (dependent variable) and several pollutant concentrations and meteorological measurements (independent variables). The first step of the EDA was to plot ozone against all of the independent variables to visualize if the data collapsed into any identifiable pattern, thus to later on use such a pattern to identify potential models. The measurements in an hourly time scale did not show any observable pattern between the dependent and independent variables as shown in Figure 3. To better understand the relations between the dependent variable and independent variables, the correlation matrixes were produced.

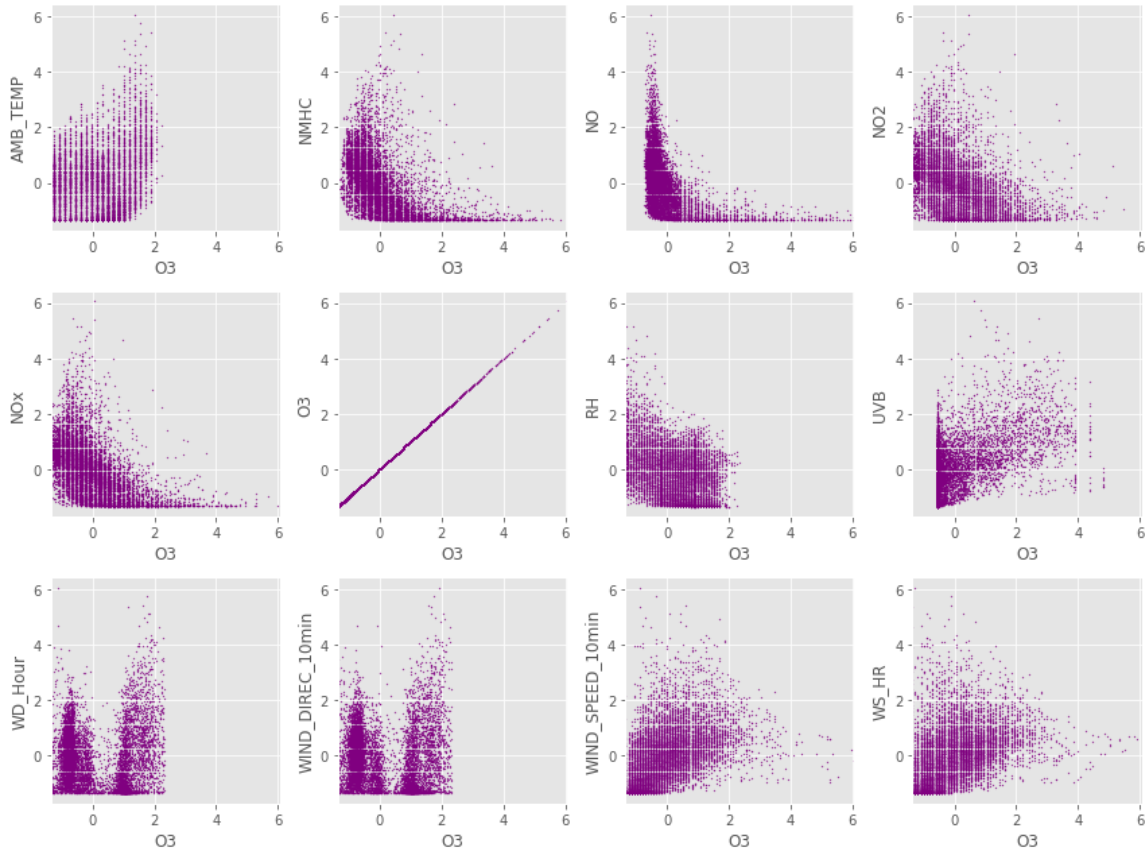


Figure 3: Scatter plots of hourly measurements of variables

Plotting the raw data, i.e. the available measurements without any processing or transformation, did not yield any insights that could help elucidate the relation between the variables. Therefore, the data was normalized. Notwithstanding, normalization did not translate into plots where patterns could be identified. Thus, the data was processed again following two consecutive steps. First the values were averaged over a day and over a month producing a dataset of daily and monthly measurement. Second, monthly and daily values were standardized by dividing them by their corresponding daily and monthly averages. As seen on figure 4, were daily standarized ozone concentrations are shown, and figures 5 6 displaying standarized pollutant monthly concentrations and metereological variables measurements.

The resulting daily and monthly standardized averages were plotted against time. Plotting the daily averaged variables shown plots were the fluctuations of the values happened in a relatively short time and thus such fluctuations obscured any pattern that could be observed in the data. These was prevalent for all variables, here we show only standarized daily ozone concentrations 4. Conversely, when the monthly standardized averages were plotted against time it was visible that the pollutants concentrations shown similar time patterns as seen in Figure 5.

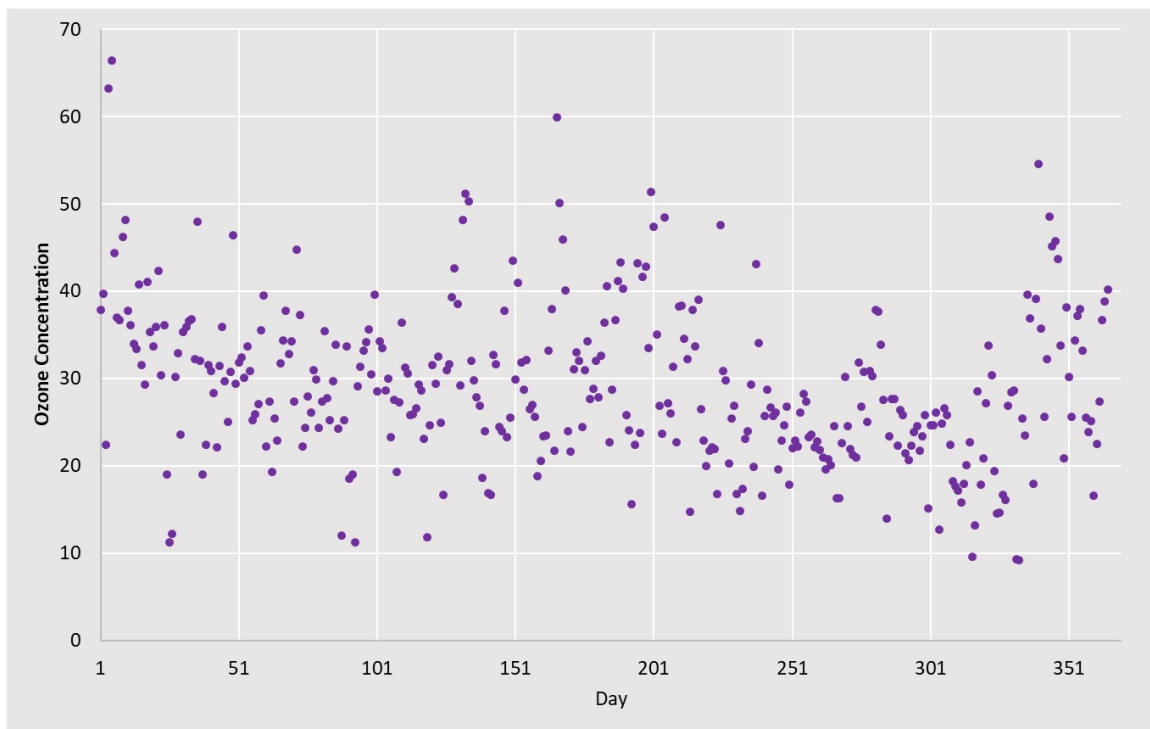


Figure 4: Daily concentrations of ozone

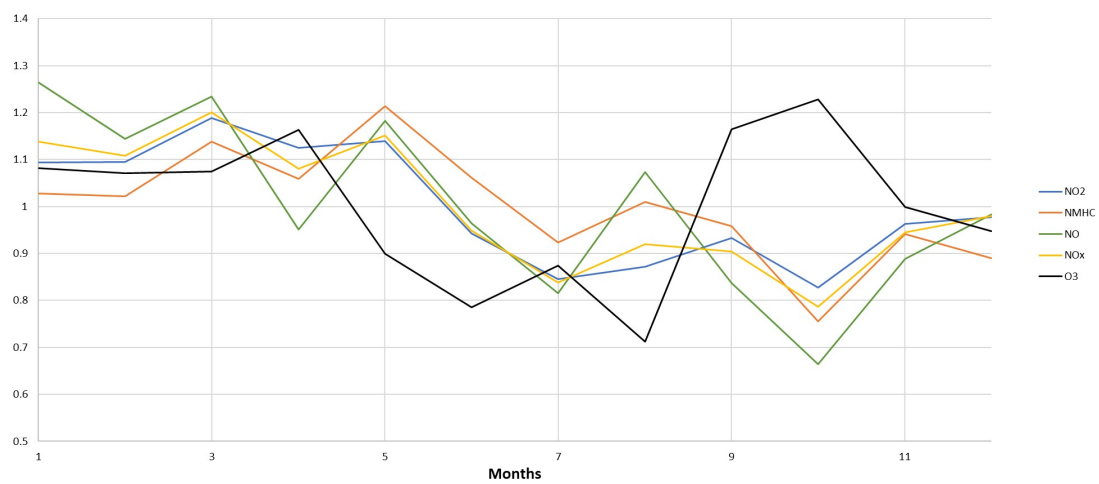


Figure 5: Standardized pollutants and ozone monthly concentration changes

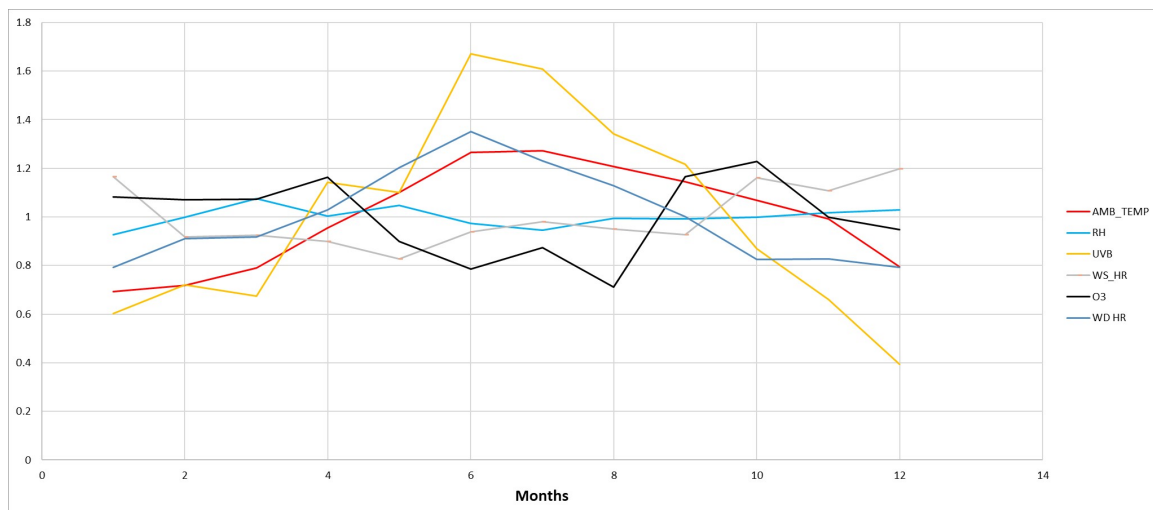


Figure 6: Standardized meteorological measurements and standardized ozone monthly concentration changes

In regards to pollutant concentrations, O₃ peaked in the months when concentration of the nitrogen based pollutants and non-methane hydrocarbons dropped. This is especially the case for NO concentrations (green line). This pattern of corresponding decreasing pollutant concentrations and increasing ozone could suggest that the pollutant concentrations are negatively correlated with ozone concentrations. This is also consistent with figure ?? (correlation plot). As shown in the figure correlation values for the nitrogen species are negative, indicating negative correlation, and vary from -0.41 to -0.5.

In regards to the meteorological variables, UVB (ultraviolet index) and air temperature peak in the same months. Both temperature and UVB experience an increase in their values from the beginning of the year peaking in June. After June, both values experience a steady decrease. In the case of UVB a positive correlation of 0.51 can be observed in ??.

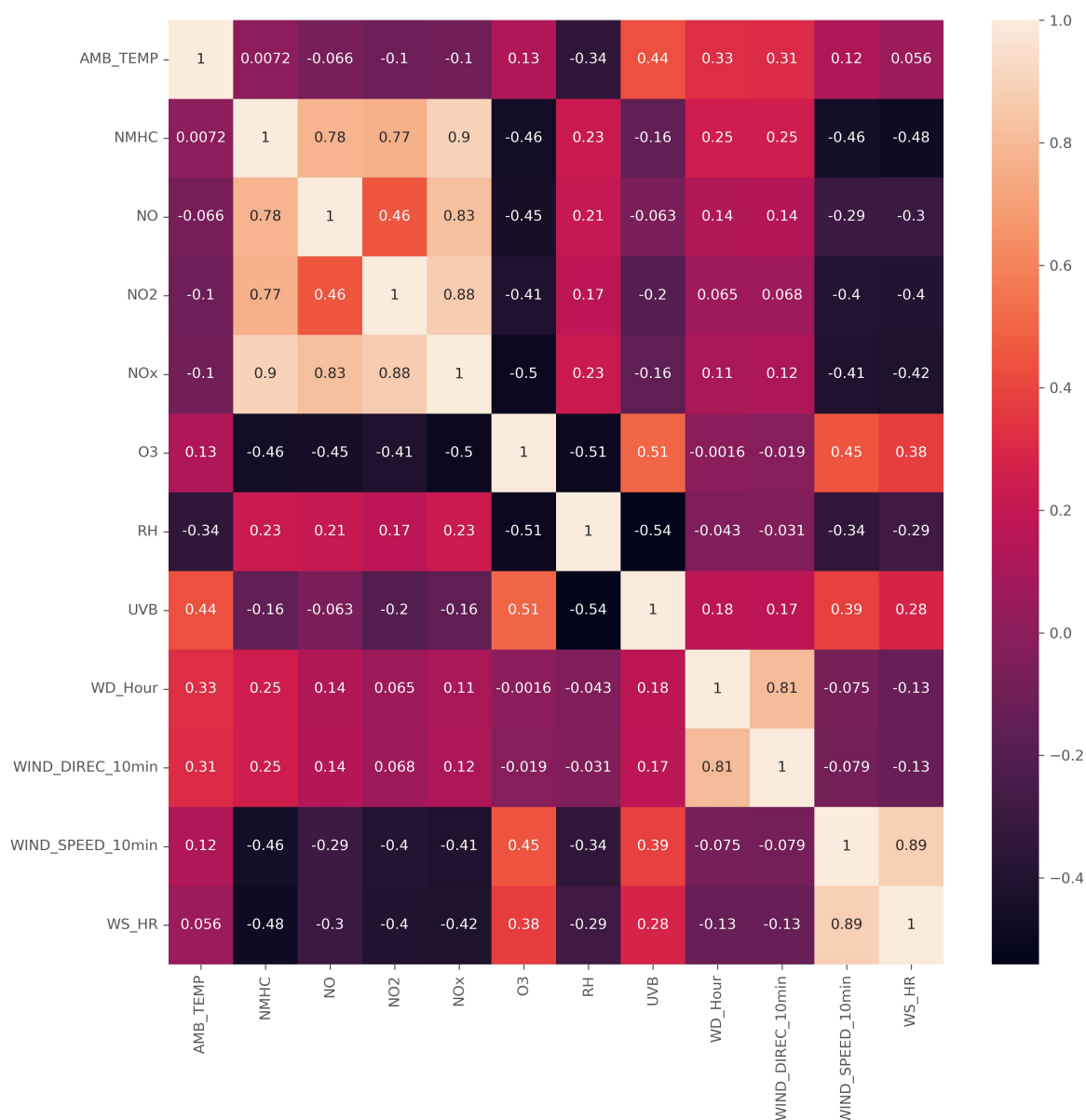


Figure 7: Correlation matrix for hourly values

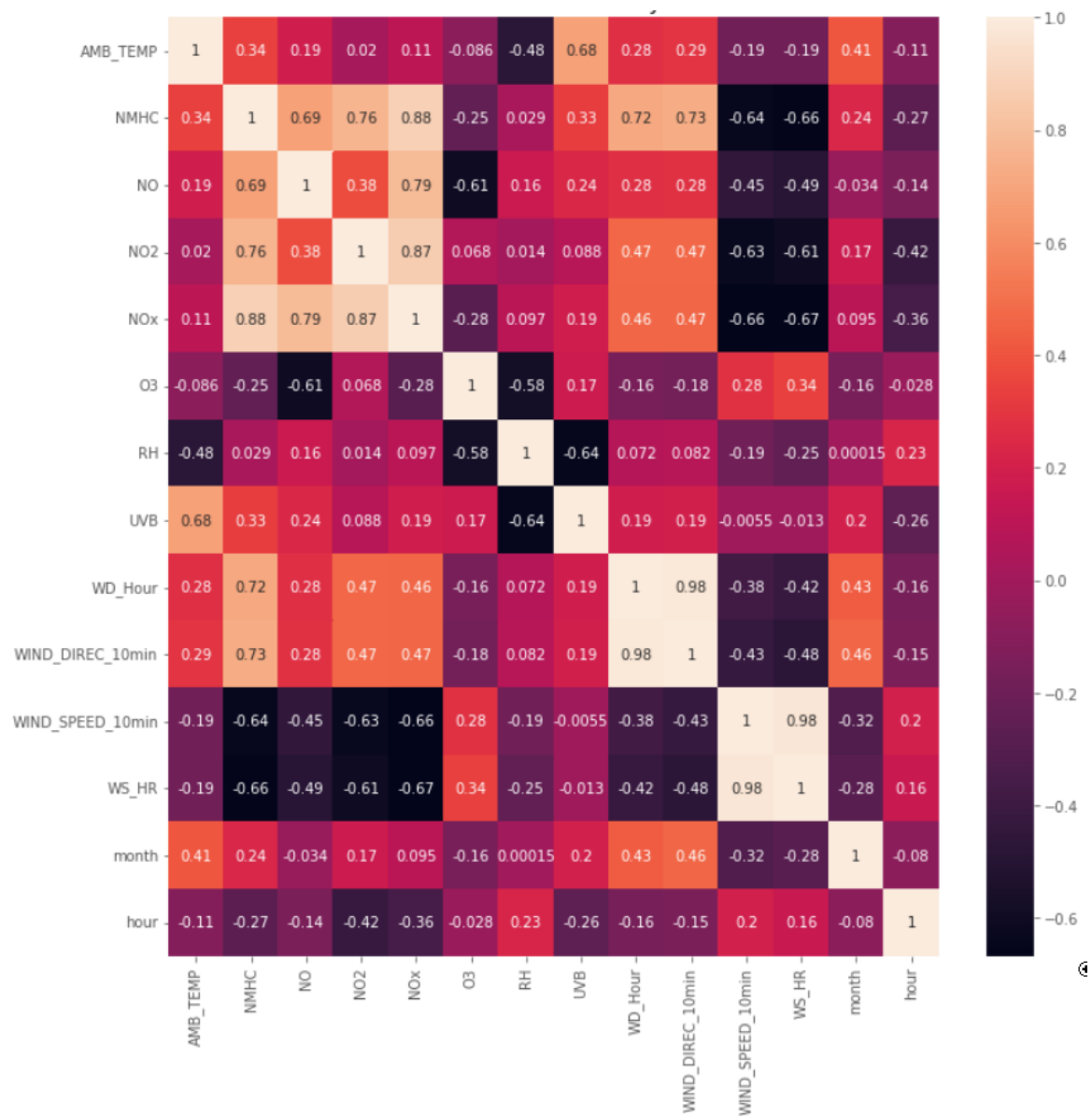


Figure 8: Correlation matrix for daily values

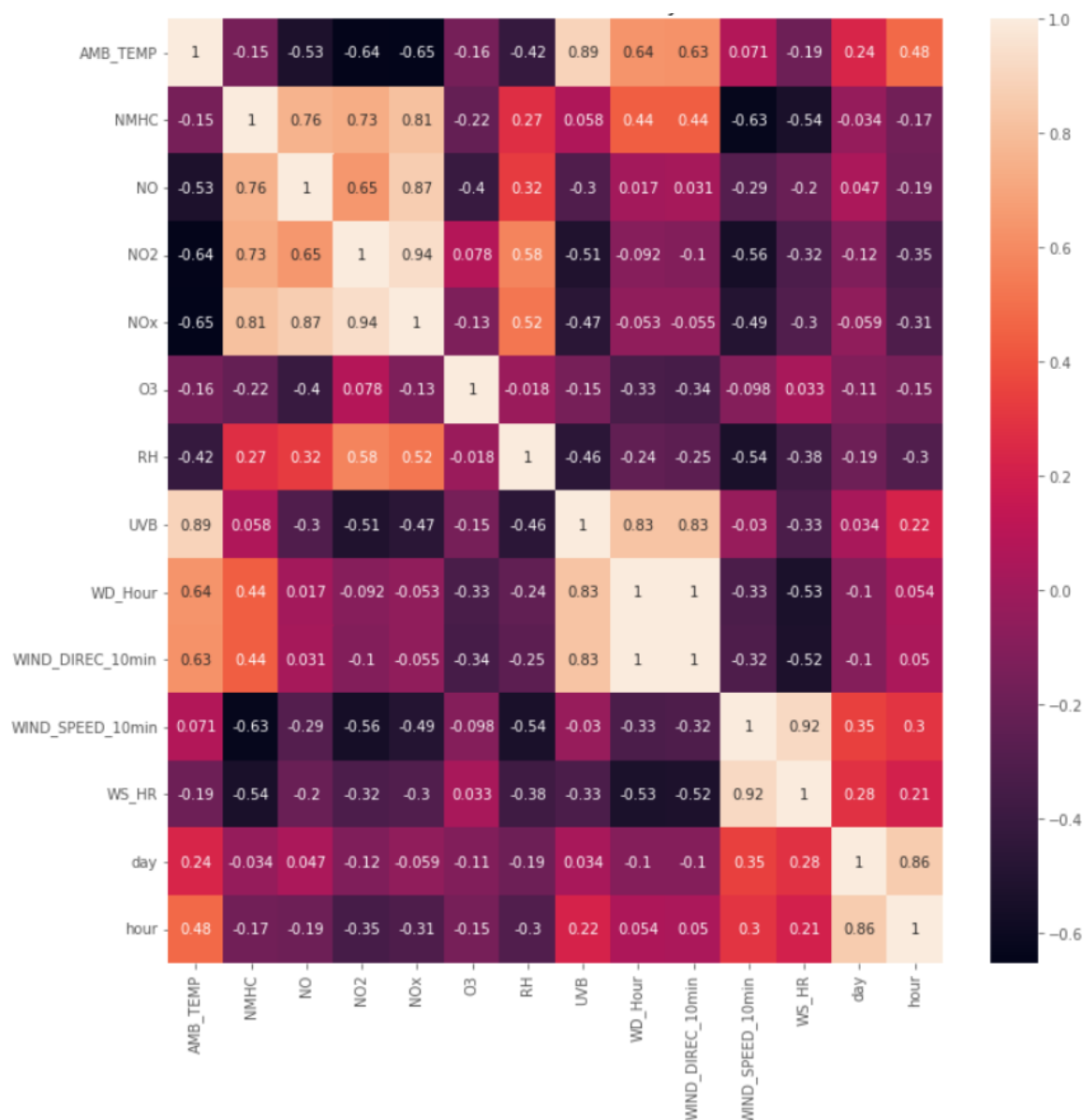


Figure 9: Correlation matrix for monthly values

Predictive Modeling

Two additional correlation matrices were produced in the previous section. One for monthly average values and another for daily average values. As observed in figures ??, [8](#), [9](#), correlation values of ozone with respect to daily and monthly values of nitrogen-containing compounds, NMHC and temperature are generally lower for daily and monthly averages compared to correlations values of hourly measurements. Consequently, the hourly measurements will be used for predictive modeling. Further discussion regarding the relation between the potential predictors and the predictand O_3 will be limited to hourly measurements only.

Values of the coefficient of determination (r^2) between O_3 and each of the other variables were generally below 0.5. This suggests a non-linear relation (most r^2 values). Given the non-linearity of the relation between the predictand O_3 and the potential predictors favoring the use of a neural network over other models such as multiple linear regression models seemed reasonable. Three different types of neural networks were tested. Additionally, a classification three model was also examined, since as seen in further section, error values of the neural network models were relatively high.

Testing of different neural network models

Different configurations of neural networks were tested. Fully connected layer neural networks, hereafter called NN, convolutional neural networks (CNN) and long short-term memory neural networks (LSTM).

In order to explain the utility of LSTMs a drawback of CNNs have to be discussed. Convolutional neural networks (CNN) use filters to extend the depth of the input volume. One drawback of CNN is that its gradients can explode or vanish which may restrict neural network performance. Long short-term memory use two path for long (cell state) and short memories (hidden state) to avoid the exploding/vanishing gradient problem.

LSTM has three gates that determined the output: forget gate to determine the percentage of long-term memory that is remembered via a Sigmoid function; input gate to calculate both the potential memory using a Tanh function and the percentage of potential memory that is remembered; and a third gate, called the output gate, to multiply a Tanh function with the long-term memory results to obtain the output.

The NN, CNN and LSTM models were used to predict hourly concentrations of O₃ (predictand or dependent variable) using as predictors the most correlated variables found in the EDA. The variables used as predictors (independent variables) were hourly measurements of: relative humidity (RH), ultraviolet radiation (UVB rays), NMHC, NO_x, NO and NO₂. In the case of LSTM ambient temperature was also used as dependent variable.

ID	Normalize	Activation function	Number of neurons	Number of Dense Layers	Epochs	η	RMSE Training	RMSE Testing
NN 1	No	Relu	18	1	1.E+03	1.0.E-04	10.4	11.7
NN 2	No	Tanh	18	1	1.E+03	1.0.E-10	15	17.3
NN 3	Yes	Relu	18	3	1.E+03	1.0.E-04	8.5	10.6
NN 4	Yes	Tanh	18	3	1.E+04	1.0.E-10	14	15.5
NN 5	Yes	Relu	18	4	1.E+03	1.5.E+00	7.5	9.9
NN 6	Yes	Relu	36-18-12	4	1.E+03	1.5.E+00	7.5	10.3
NN 7	Yes	Relu	18	5	1.E+03	1.5.E+00	7	9.8
NN 8	Yes	Relu	18	8	2.5.E+03	1.5.E+00	6.4	9.2

Figure 10: RMSE values for different hyperparameters and NN configurations

ID	Normalize	Activation function	Number of neurons	Number of Convolutional Layers	Number of Dense Layers	Epochs	η	RMSE Training	RMSE Testing
CNN 1	Yes	Relu	12	1	2	1.E+02	1.E-02	10	10.2
CNN 2	Yes	Relu	18	1	2	1.E+02	1.E-02	9.3	9.5
CNN 3	Yes	Relu	36	1	2	1.E+02	1.E-03	9.5	9.6
CNN 4	Yes	Tanh	18	1	2	1.E+02	1.E-02	12.3	13.5
CNN 5	Yes	Relu	18	1	2	1.E+02	1.E-02	9.1	9.4
CNN 6	Yes	Relu	18	1	2	3.E+02	1.E-02	9.2	9.1
CNN 7	Yes	Relu	18	1	2	5.E+02	5.E-05	4.7	7.7
CNN 8	Yes	Relu	18	2	2	3.E+02	5.E-05	4.8	7.2
CNN 9	Yes	Relu	18	3	2	2.E+02	5.E-05	1.8	9.0

Figure 11: RMSE values for different hyperparameters and CNN configurations

Different combinations of hyperparameters were tested. Model predictive ability was measured using the root mean square error (RMSE) for training and testing data. The results of such tests are summarized in [11](#) and [10](#). A similar table detailing RMSE for different combinations of numbers of memory cells and hidden layers on LSTM was not produced since training time neared 3 hours, yet based on trial and error a configuration of 2 LSTM layers of 32 and 64 neurons and 2 dense layers was

selected. Values of RMSE were computed both for training and testing data. For all the models, including neural networks and classification tree, a 0.7 fraction of the dataset was used for training and the remaining 0.3 was used for testing.

When looking at [11](#) and [10](#), in all cases (NN2, NN4 and CNN4)the best performing activation function was rectified linear unit (ReLu) when compared to hyperbolic tangent. Therefore, ReLu was used as activation function for the rest of tests. In NN 4 the number epochs was increased by one order of magnitude since neural network outputted a significantly higher RMSE when using the original number epochs.

Increasing the number of neurons did not decrease either RMSE in training or testing data (NN5 vs NN6) in the case the fully connected neural networks. When analyzing the CNNs, increasing the number of neurons from 12 to 18 (CNN 1 vs CNN 2) reduced testing and training RMSE. Yet when increasing to 36 neurons (CNN 2 vs CNN 3) both training and testing RMSE increased. It is necessary to mentioned that the learning rate was reduced for CNN 3 to prevent NaN outputs. For additional tests on CNNs, 18 neurons were used, since it seemed to be the configuration that yielded the best results on terms of RMSE.

Number of layers reduce both RMSE for training and testing both for NN. However, RMSE on training data dropped more significantly for training data than for testing data. This might indicate a tendency towards overfitting the training data using NN on this dataset. In the case of CNN, when increasing the number of convolutional layers ,RMSE increased marginally for training data and drop for testing data (CNN7 vs CNN8). When adding another convolutional layer (CNN8 vs CNN9) training RMSE dropped significantly (overfitting) and testing RMSE increased, suggesting poor generalization. Additional figures, shown bellow, showing the influence of number epochs used in training on RMSE were created.

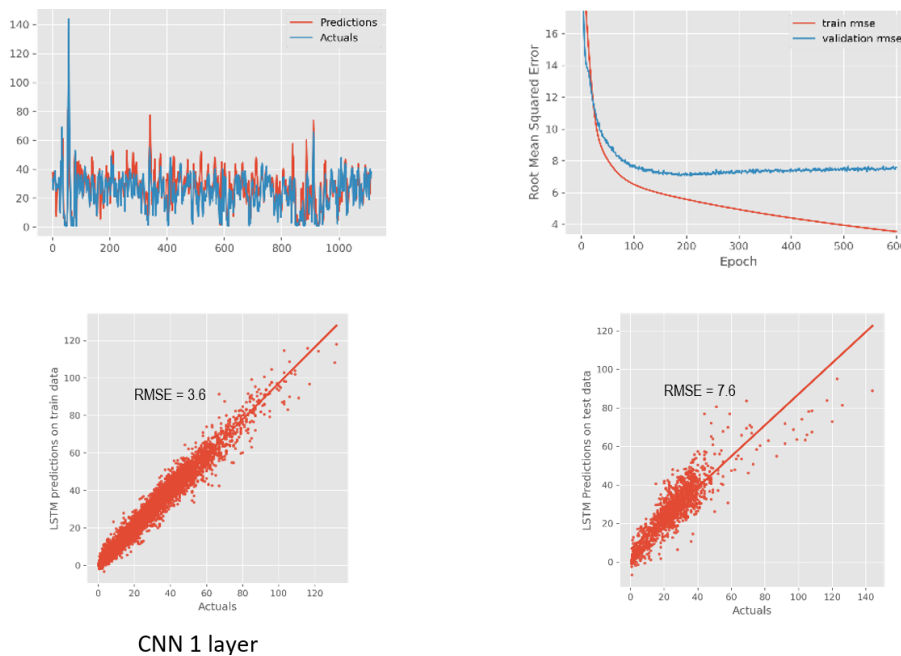


Figure 12: Training and testing RMSE versus number of epochs and predictions versus observations (actual values) for LSTM

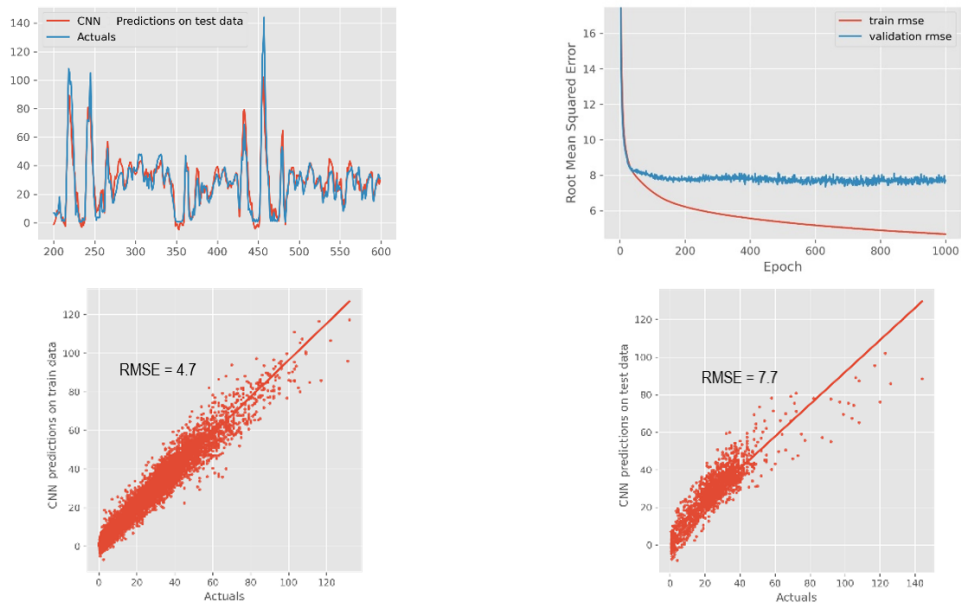


Figure 13: Training and testing RMSE vs number of epochs and predictions versus observations for CNN 7 (1 layer CNN)

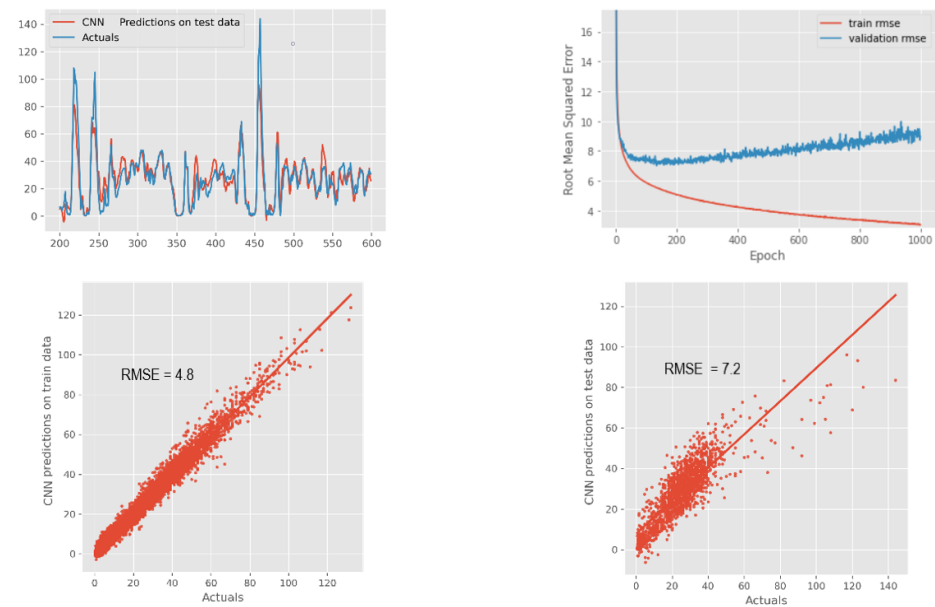


Figure 14: Training and testing RMSE vs number of epochs and predictions versus observations for CNN 8 (2 layer CNN)

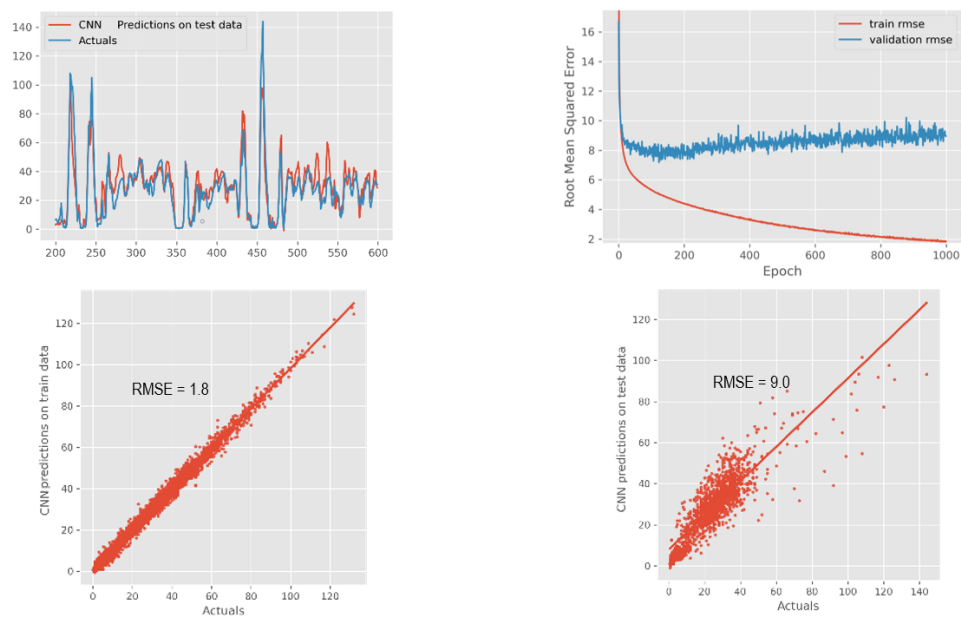


Figure 15: Training and testing RMSE vs number of epochs and predictions versus observations for CNN 9 (3 layer CNN)

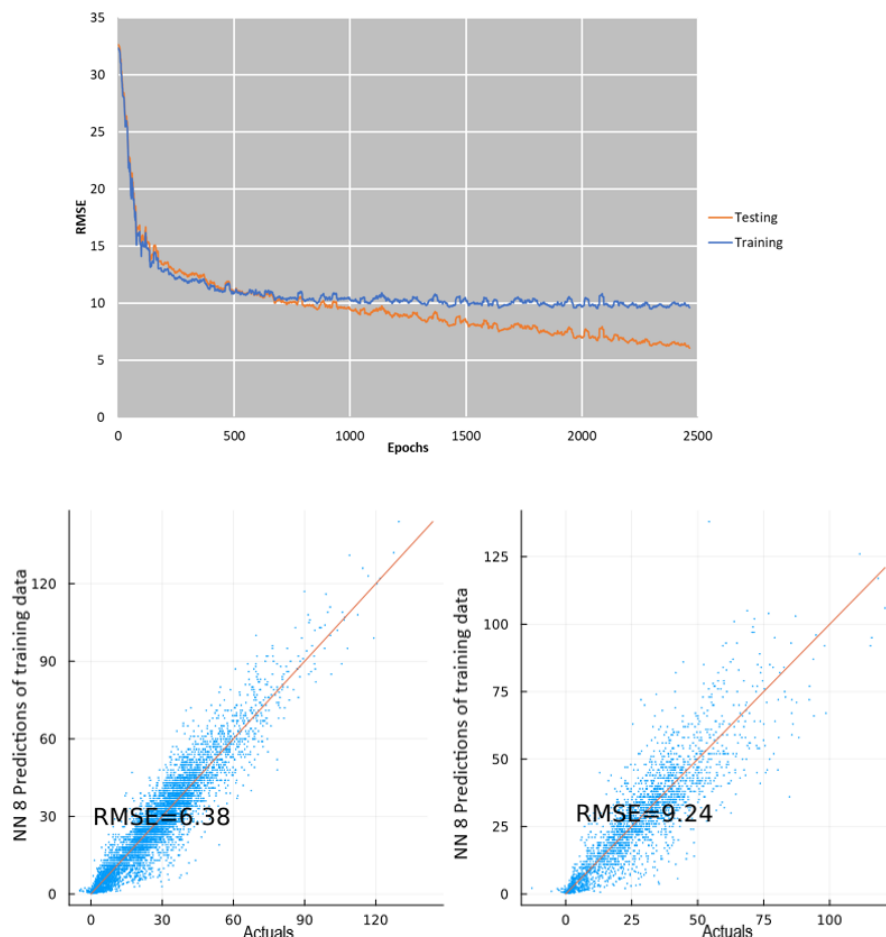


Figure 16: Training and testing RMSE vs number of epochs and predictions versus observations for NN 8 (8 layer NN)

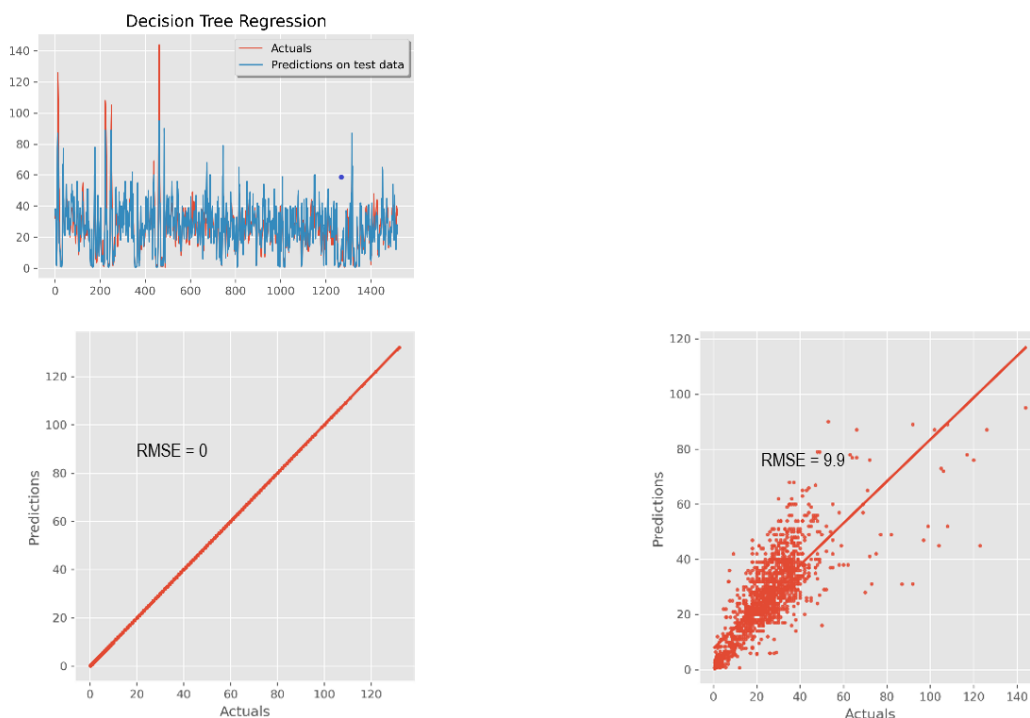


Figure 17: Training and testing RMSE and predictions versus observations for classification tree

Another important aspect is the effect of the number of training epochs on RMSE. In all the cases, [16](#), [13](#), [14](#), [15](#), RMSE for the training data dropped with increased number of epochs. However, RMSE for testing data initially dropped from the epoch 1 to 300 and then increased for LSTM ([12](#)) and CNN 2

and 3 ([14](#), [15](#)) for additional training steps. In the cases of CNN 1([13](#)) and NN 8 ([16](#))RMSE for testing data continued to drop, but at a lower rate than RMSE for training data. Because of most of the cases either RMSE increased with increased number of epochs or RMSE reduction was modest in comparison to increased training time, number of epochs was limited to 2500 for NN 8, 300 for CNN 8 and 300 for LSTM. In the case of the classification tree model, [17](#), RMSE is zero for the training data, where as RMSE for testing data is 9.9. This is by far the most extreme example of overfitting of all the models.

Discussion

The lowest RMSE measured in all the different neural network-based model was 7.7 PPB (CNN 8). For reference, the mean value of ozone concentration in the dataset was 25.0 PPB, thus the level of error of the predictive model might be deemed unsatisfactory. This motivated to test a classification tree model. RMSE for the classification tree was 9.7 PPB, which is greater than the lowest RMSE yielded by the neural network models.

The original goal of this project was to predict O₃ using measurements of other compounds and meteorological variables. Since the error value of the model predictions are high compared to the values of the measured concentrations of O₃ it can assumed that ozone concentrations can be predicted yet predictions will have a significant error value associated with them. Being these a related potential path for future work could be suggested.

The model question could be refined from “can ozone concentrations be predicted using the available data” to “can the available dataset be used to predict when ozone concentrations will exceed 70 PPB?”. This value is the threshold of the primary (public health) and secondary (public welfare) 8-hour ozone standards defined by the “2015 Revision to 2008 Ozone National Ambient Air Quality Standards (NAAQS) Related Documents”. Thus, by refining the research question the modeling effort will transition from a regression / prediction model to a binary classification model which might be a more error tolerant goal.

References

Reference: <https://machinelearningmastery.com/return-sequences-and-return-states-for-lstms-in-keras/>

<https://machinelearningmastery.com/stacked-long-short-term-memory-networks/>

https://en.wikipedia.org/wiki/Convolutional_neural_network#Convolutional_layer

<https://www.youtube.com/watch?v=YCzL96nL7j0> "Long Short-Term Memory (LSTM), Clearly Explained"

<https://www.youtube.com/watch?v=kGdbPnMCdOg> "Multivariate Time Series Forecasting Using LSTM, GRU & 1d CNNs"

<https://github.com/Dana2021/CEE498DS-Project1>

https://blog.csdn.net/bryan_/article/details/51607215 "Introduce several common feature selection methods in conjunction with Scikit-learn"